Am J Physiol Cell Physiol 285: C1386–C1396, 2003.
First published August 13, 2003; 10.1152/ajpcell.00338.2002.

VACM-1, a cul-5 gene, inhibits cellular growth by a mechanism that involves MAPK and p53 signaling pathways

C. Van Dort,[1] P. Zhao,[2] K. Parmelee,[1] B. Capps,[1] A. Poel,[1] L. Listenberger,[1] J. Kossoris,[1] B. Wasilevich,[1] D. Murrey,[1] P. Clare,[3] and M. Burnatowska-Hledin[1]

[1]*Departments of Biology and Chemistry, Peale Science Center, Hope College, Holland, 49422-9000;* [2]*Van Andel Research Institute, Grand Rapids 49503; and* [3]*Pfizer Co., Kalamazoo, Michigan 49007*

Submitted 22 July 2002; accepted in final form 25 July 2003

Van Dort, C., P. Zhao, K. Parmelee, B. Capps, A. Poel, L. Listenberger, J. Kossoris, B. Wasilevich, D. Murrey, P. Clare, and M. Burnatowska-Hledin. VACM-1, a cul-5 gene, inhibits cellular growth by a mechanism that involves MAPK and p53 signaling pathways. *Am J Physiol Cell Physiol* 285: C1386–C1396, 2003. First published August 13, 2003; 10.1152/ajpcell.00338.2002.—Vasopressin-activated Ca^{2+}-mobilizing (VACM)-1 gene product is a 780-amino acid membrane protein that shares sequence homology with cullins, a family of genes involved in the regulation of cell cycle. However, when expressed in vitro, VACM-1 attenuates basal and vasopressin- and forskolin-induced cAMP production. Mutating the PKA-dependent phosphorylation site in the VACM-1 sequence (^{S730A}VACM-1) prevents this inhibitory effect. To further examine the biological role of VACM-1, we studied the effect of VACM-1 and ^{S730A}VACM-1 proteins on cellular proliferation and gene expression in Chinese hamster ovary and COS-1 cells. Cellular proliferation of VACM-1-expressing cell lines was significantly lower compared with that of the vector-transfected cells, whereas it was significantly increased in ^{S730A}VACM-1-derived cell lines. Furthermore, expression of VACM-1 but not ^{S730A}VACM-1 protein retarded cytokinesis and prevented MAPK phosphorylation. Screening with the Human PathwayFinder-1 GEArray system and subsequent Western blot analysis demonstrated that VACM-1 induces p53 mRNA and protein expression. In summary, VACM-1 inhibits cellular growth by a mechanism that involves cAMP, MAPK phosphorylation, and p53 expression.

mitogen-activated protein kinase; cytokinesis; vasopressin-activated calcium-mobilizing receptor

THE GENE for the vasopressin-activated Ca^{2+}-mobilizing (VACM-1) receptor was isolated from a rabbit kidney cDNA library and encodes a 780-amino acid protein with an estimated M_r of 91 kDa (4). Whereas the biological function of VACM-1 appears to be linked to that of arginine vasopressin (AVP) (4), its sequence is homologous with that of cullins, a conserved multigene family of intracellular proteins that regulate cellular growth and apoptosis through diverse mechanisms (17, 21). Cul-1, for example, regulates cell cycle transitions that involve two distinct ubiquitinylation pathways. As a component of the ubiquitin ligase known as SCF complex (for Skp1-cullin-F box), cul-1 is involved in the cdc34-dependent degradation of Sic1p, an inhibitor of G_1 cyclin-dependent kinase, which pushes cells into the S phase (21, 22). As a subunit of the anaphase-promoting complex involved in the degradation of the regulatory protein Pds1p, cul-1 may be involved in the regulation of metaphase-to-anaphase transitions (11, 34, 35). Cul-2, on the other hand, is a tumor suppressor candidate (27) and associates with a cellular protein complex composed of the von Hippel-Lindau gene product and elongins B and C (VBC). The VBC-Hs-cul-2 complex shuttles in and out of the nucleus, possibly degrading specific cell cycle-dependent proteins (15, 19, 25, 27). The biological roles of the recently cloned Hs-cul-3 and Hs-cul-4 genes, expressed in cultured colon cancer cells and primary breast cancer cells, respectively (8, 9), remain to be elucidated. Little is known about the biological function of Ce-cul-5, which shares 96% sequence homology at the carboxyl terminus (156/163 amino acids) with mammalian VACM-1 (6, 17) but may be biologically divergent from other cullins (5, 6, 14, 28). Only recently has cul-5 been shown to form ubiquitin ligase complexes that are involved in adenovirus-induced p53 degradation in vitro (28).

Our search to identify biological role(s) for the VACM-1 protein yielded results that clearly distinguish it from both AVP-dependent functions and cullins characterized to date (2–5) and supports a unique biological role for VACM-1, and thus for the cul-5 family. We have shown that unlike cul-1, which is expressed in most cells (17, 21), expression of VACM-1 protein in vivo is localized exclusively to specific endothelial cells (3). In the kidney, in addition to being present in vascular endothelial cells, VACM-1 is also expressed in the medullary collecting tubule cells, structures involved in AVP-dependent regulation of water and solute transport (3, 4, 13). When expressed in vitro, VACM-1 protein binds AVP (K_d = 2 nM) but not the V_1 or V_2 receptor-specific analogs and regulates basal Ca^{2+} concentration (4). Furthermore, VACM-1 cDNA expression in Chinese hamster ovary (CHO) and COS-1 cells attenuates basal as well as forskolin- and AVP-dependent cAMP signaling (2). The ability of

Address for reprint requests and other correspondence: M. Burnatowska-Hledin, Dept. of Biology, Peale Science Center, Hope College, Holland, MI 49422-9000 (E-mail: Hledin@hope.edu).

The costs of publication of this article were defrayed in part by the payment of page charges. The article must therefore be hereby marked "*advertisement*" in accordance with 18 U.S.C. Section 1734 solely to indicate this fact.

 0363-6143/03 $5.00 Copyright © 2003 the American Physiological Society

VACM-1 to attenuate the AVP- and forskolin-induced production of cAMP depends on its phosphorylation status, which is regulated by protein kinase A (PKA) and protein kinase C (PKC) (2). The inhibitory effect of VACM-1 on cAMP production can be reversed by mutating the PKA-dependent phosphorylation site in its sequence (^{S730A}VACM-1) (2).

Unlike the membrane-integrated AVP receptors (13) or the cytosolic/nuclear cul-1 and cul-2 proteins (17, 22, 27), VACM-1 can be either nuclear/cytosolic or a cell membrane protein (4, 5). Furthermore, the expression of VACM-1 protein and/or its translocation to the cell membrane is dependent on the specific stages of the cell cycle (5). In nonproliferating and in aphidicolin-arrested (G_0) cells derived from rat adrenal medullary endothelial cells (RAMEC) (26), VACM-1 expression localizes to the cell membrane. During the S phase, however, VACM-1 protein virtually disappears from the cell, and at the onset of mitosis, VACM-1 localizes to the nuclear region. At the completion of cytokinesis, VACM-1 presence in the cell membrane is evident again (5). This pattern of cellular distribution is clearly different from that shown for cul-1, which remains stable throughout the cell cycle (22). Although the biological significance and the mechanism of VACM-1 protein translocation between the nucleus and the cell membrane are not clear at present, the effect of VACM-1 on the AVP-dependent changes in the cytosolic free Ca^{2+} can only be observed when VACM-1 localizes to the cell membrane (5). VACM-1, therefore, appears to be the first example of a cell cycle-dependent protein that translocates from the cytosol/nucleus to the membrane and regulates basal and hormone-dependent Ca^{2+} and cAMP signaling pathways (2, 5).

Because both Ca^{2+} and cAMP signaling pathways have been implicated in the regulation of cellular proliferation (10, 18, 32), we have extended our studies to examine the effects of VACM-1 cDNA expression on cellular growth. We report here that stable expression of VACM-1 in CHO and COS-1 cells attenuated cellular proliferation, whereas the expression of ^{S730A}VACM-1 mutant significantly increased cellular growth by a mechanism that regulates MAPK phosphorylation. Finally, screening a Human Pathway-Finder-1 GEArray with the use of cRNA probes from control and VACM-1 cDNA-transfected COS-1 cells and subsequent Western blot analyses indicated that expression of VACM-1 in COS-1 cells regulates p53 mRNA and protein expression. In summary, our results support the role of VACM-1 protein in the regulation of cellular growth that involves regulation of MAPK phosphorylation and p53 gene expression.

MATERIALS AND METHODS

Materials. All tissue culture media and reagents were purchased from GIBCO (Grand Island, NY). [^{32}P]ATP and [^{3}H]AVP were purchased from DuPont-NEN (Boston, MA). Restriction enzymes were purchased from Promega (Madison, WI).

Tissue culture. CHO and COS-1 cells were grown in F-12 and DMEM media, respectively, supplemented with 10% FBS at 37°C under a water-saturated 7% CO_2 atmosphere as described previously (4). Cells were subcultured for 24 h before transfection at a density of 6×10^5 cells per 100-mm plate. Cells were transfected with 5 μg of VACM-1 cDNA per 100-mm culture dish, using the DEAE-dextran method for the CHO cells and FuGENE 6 (Roche Diagnostics, Indianapolis, IN) for the COS-1 cells. For the stable expression of VACM-1 cDNA in DHG44-CHO dhfr − cells, EMC3 vector (kindly donated by the Genetic Institute, Cambridge, MA) was used. VACM-1 cDNA was cut with unique *Sal*I/*Xba*I restriction enzymes from the pSV-SPORT-1 vector and ligated into the *Sal*I/*Xba*I site in the polylinker region of EMC3 vector upstream from the dihydrofolate reductase (dhfr) gene, allowing coamplification of the dhfr and VACM-1 cDNAs. On the basis of a single-point [^{3}H]AVP binding assay and an increase in Ca^{2+} in response to AVP, we identified three clone lines expressing VACM-1 receptor. The cells were cloned by limited dilution, several clones were isolated, and clone A was chosen for all subsequent studies. COS-1-derived stable cell lines were established by transfecting COS-1 cells with VACM-1 cDNA subcloned into the *Sal*I/*Not*I restriction site in the polylinker region of pBK-CMV vector (Stratagene, La Jolla, CA). After 24 h, cells were split and incubated with fresh medium containing 600 μg/ml G418 (GIBCO BRL, Gaithersburg, MD). The medium was changed every 3 days. Two weeks after transfection, G418-resistant cells were harvested and transferred into six-well plates containing selective medium (250 μg/ml G418). Ultimately, seven clones were isolated and characterized.

Northern blot analysis. Poly(A^+) mRNA was isolated by the C Fast Track method. Varying concentrations of poly(A^+) mRNA were separated on a 1% agarose gel containing 16% formaldehyde, transferred to a nitrocellulose membrane, and fixed by baking under vacuum at 80°C for 1 h. The mRNA blot was prehybridized for 1 h at 42°C in a solution containing 50% formamide, 2× SSC, 5× Denhardt's solution, 0.1% SDS, and 100 μg/ml denatured salmon sperm DNA. The hybridization was performed for 24 h at 42°C in 50% formamide, 2× SSC, 1× Denhardt's solution, 100 μg/ml denatured salmon DNA, and 2×10^6 counts/ml of the ^{32}P-labeled *Eco*RI/*Bcl*I fragment of VACM-1 cDNA (nt 355–1245). After hybridization, the Northern blot was washed twice in 1× SSC and 0.1% SDS at room temperature and twice in 0.1× SSC and 0.1% SDS at 45°C (30 min each) and then examined by autoradiography. Blots were reprobed with a GAPDH probe to standardize for equal RNA loading (4).

Total cell lysate preparation. Cells were grown to 70% confluency, washed in ice-cold PBS, and resuspended in 500 μl of buffer (50 mM Tris, pH 7.4, 0.1% Triton X-100, 150 mM NaCl, 1 mM EDTA, and 50 mM NaF) with 1 μg/ml apoprotein, 100 μM Pefabloc SC, and 10 mM PMSF. All samples were homogenized with a Polytron homogenizer, and protein concentration was determined using the Bradford method (Bio-Rad, Richmond, CA).

Immunoprecipitation. Cell lysates (300 μg of protein) were resuspended in 150 μl of solubilization buffer (50 mM Tris·HCl, pH 8, 150 mM NaCl, 0.3% Triton X-100, 1 mM Pefabloc SC, and 10 μg/ml aprotinin) and incubated with a 1:250 dilution of affinity-purified antibody A (Ab A), directed against the amino-terminal sequence of VACM-1 protein. After 2 h of incubation at 4°C, an equal volume aliquot of protein A-Sepharose (Amersham Pharmacia Biotech) suspension was added and the incubation continued for another 2 h. The complex was centrifuged at 12,000 rpm for 2 min and washed two to three times in the solubilization buffer. Loading dye (Invitrogen) was added, and the immunoprecipitates were separated by SDS-PAGE using Novex gels (Invitrogen),

transferred to nitrocellulose, and probed with an antibody directed against NEDD8 protein (Alexis Biochem) as described below.

Western blot analysis. Total cell lysates prepared as described were resuspended in 2× sample buffer (Bio-Rad), heated to 95°C for 4 min, and subjected to SDS-PAGE using a 10% running gel. The separated proteins were transferred to nitrocellulose membranes at 30 mV overnight. Nonspecific sites were blocked by membrane incubation for 30 min at room temperature with PBS containing 5% nonfat dry milk and 0.2% Tween 20. Membranes were incubated for 2 h at room temperature in buffer solution containing a 1:200 dilution of affinity-purified polyclonal antibodies directed against either the amino terminus (Ab A) or the carboxyl terminus (Ab B) of VACM-1 protein (3, 4) or a 1:500 dilution of anti-p53 antibody. Total MAPK levels were assessed with anti-ERK1 and anti-ERK-2 antibodies (Transduction Labs, Lexington, KY). PhosphoPlus MAPK antibody, which detects phosphorylated tyrosine 204 and threonine 202 of p44 and p42, was used in subsequent studies (1:500 dilution; Cell Signaling Technology, Beverly, MA). Next, the membranes were washed in the same buffer for 15 min and twice for 5 min and then incubated for 2 h with a 1:10,000 dilution of a horseradish peroxidase-conjugated anti-rabbit antibody (Cell Signaling Technology). The nitrocellulose membranes were washed as described above, exposed to the luminol detection reagents (Cell Signaling Technology) for 1 min, and then exposed to the X-ray film (Amersham Pharmacia Biotech).

Immunostaining. Affinity-purified polyclonal antibodies directed against the amino terminus (Ab A) of VACM-1 protein characterized previously (4) were used to stain cells grown on coverslips by indirect immunofluorescence. Cells grown on coverslips were fixed in 3% paraformaldehyde (in 1× PBS, pH 7.4), washed in PBS, and incubated with a 1:20 dilution of Ab A or of Ab A preabsorbed with 10 μM peptide A, identical in sequence to the amino-terminal sequence of VACM-1, in PBS containing 0.1% BSA (PBS/BSA) for 1 h. Cells probed with anti-p53 antibody (1:80 dilution) were first permeabilized with 5% Tween 20 solution for 20 min, washed with PBS/2% BSA, and exposed to p53 antibody as described for Ab A. The primary antibodies were detected by incubating the sections in the presence of a 1:40 dilution of FITC-conjugated goat anti-rabbit IgG or anti mouse IgG (Vector Laboratories, Burlingame, CA) in 1× PBS/2% BSA for 1 h. Nuclear staining was achieved by 4,6-diamidino-2-phenylindole (DAPI), found in the Vectashield mounting medium (Vector Laboratories). Sections were washed in 1× PBS/2% BSA, mounted with either Aqua Polymount (Polysciences, Warrington, PA) or Vectashield, and viewed by epifluorescence microscopy (BH2; Olympus, Lake Success, NY).

Cellular proliferation assays. Clone A and control CHO cells were seeded in 24-well plates at equal densities (2×10^4 cells/ml) in 10% FBS. After 24 h, medium was changed and cells were allowed to grow for 72 additional hours. The Cell Titer Nonradioactive Cell Proliferation Assay from Promega was used to determine the number of viable cells. Control COS-1 cells transfected with CMV vector and COS-1-derived lines, also seeded at equal density (2×10^4 cells/ml), were harvested by trypsinization and counted in a hemacytometer. In addition, some cells were grown on coverslips and stained with DAPI as described, and nuclei visualized under epifluorescence microscopy were counted.

Fluorescence-activated cell sorting analysis. CHO and clone A cells were harvested after treatment with aphidicolin (1.25 μg/ml) for 16 h. Cells were washed in PBS, centrifuged, and then fixed in ice-cold 90% ethanol for at least 4 h. Before analysis, samples were washed with PBS and resuspended in a solution containing 40 μg/ml propidium iodide (PI) and 200 μg/ml RNase A in PBS and incubated at 4°C for at least 15 min. Samples were analyzed using a Becton Dickinson FACScan flow cytometer using the ModFit LT 2.0 program from Verity Software House. Ten thousand events were collected for each sample, and the resulting histograms were analyzed for the percentage of cells in each cell cycle phase (5, 29).

Microarray assay. A Human PathwayFinder-1 GEArray Kit obtained from SuperArray (Bethesda, MD) was probed with biotin-16-dUTP-labeled VACM-1 cRNA and exposed to the AP-streptavidin chemiluminescent detection system exactly as described in the manufacturer's instructions.

Statistical analysis. Kodak Digital Science 1D LE 3.0 was used to scan the Western blot results, and the NIH Scion Imaging program was used for analysis. Data are expressed as means ± SE. A Student's *t*-test was used to compare means. Significance was set at $P < 0.05$.

RESULTS

To characterize VACM-1 protein, we established three stable transformants in CHO cells and used clone A in subsequent studies. Visual examination under light microscopy indicated that cells transfected with VACM-1 cDNA grew more sparsely than control cells seeded at the same density (Fig. 1*A*, *a–b*). VACM-1 protein expression was confirmed by immunostaining the control and VACM-1-expressing cells (clone A) with anti-VACM-1-specific antibody (Fig. 1*A*, *c–d*) and by Western blot analysis (Fig. 1*B*). A total cell lysate from RAMEC expressing endogenous VACM-1 (5) was used as a positive control. The inhibitory effect of VACM-1 expression on cellular growth was further confirmed using a proliferation assay kit (Fig. 1*C*).

Because of VACM-1 sequence homology with cullins, which interact with proteins known to regulate the course of cell cycle, we wanted to test the hypothesis that expression of VACM-1 protein alters cellular progression through the cycle. Control and VACM-1-transfected CHO cells, grown to ~50% confluency, were arrested with an inhibitor of DNA polymerase, aphidicolin (1.25 μg/ml) (5, 31). The progression of cells through the cell cycle, at 0, 4, 8, 12, and 24 h after release from the aphidicolin treatment, was monitored by fluorescence-activated cell sorting (FACS) analysis. These data, summarized in Fig. 1*D*, demonstrate that CHO cells completed their progression through the cell cycle within 12 h after the removal of aphidicolin block, whereas cells overexpressing VACM-1 protein appeared to have completed a cycle of cell division only by 24 h.

To confirm and further extend these observations, we next established several VACM-1 stable cell lines in COS-1 cells. To visualize VACM-1 protein localization in COS-1-derived cell lines, the immunocytochemistry of control and representative *clone 1* cells were performed using antibodies generated against the carboxyl terminus of VACM-1 protein, characterized previously (3, 4). To identify the stages of the cell cycle, we performed nuclear staining with DAPI. Data for the *clone 1* cells indicate that during anaphase, VACM-1 protein localized to the nucleus (Fig. 2*A*, *a–b*). Cells overexpressing VACM-1 protein completed the S phase

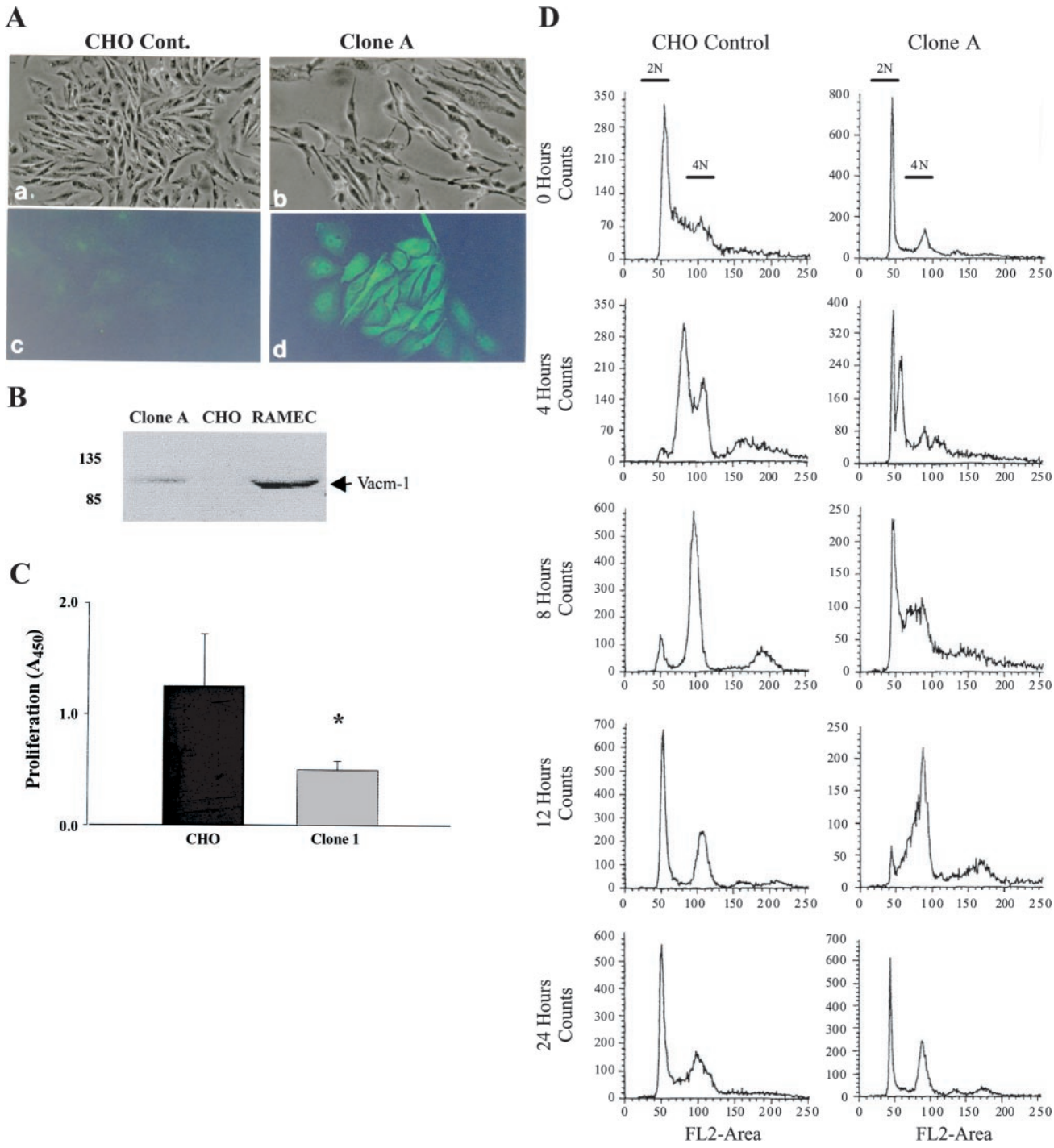


Fig. 1. Effects of vasopressin-activating Ca^{2+}-mobilizing (VACM-1) receptor cDNA expression on cellular growth in Chinese hamster ovary (CHO) cells. *A*: phase-contrast (*a* and *b*) and immunocytochemistry (*c* and *d*) images of control CHO cells (*a* and *c*) and CHO cells stably transfected with VACM-1 cDNA (*b* and *d*). Cells were grown on coverslips, fixed, permeabilized, and immunostained with anti-VACM-1 antibody. No VACM-1 expression was observed in cells immunostained with the antibody preincubated with 10 μg of peptide (not shown). *B*: Western blot analysis of VACM-1 protein expression in CHO and clone A cells relative to endogenous VACM-1 expression in rat adrenal medullary endothelial cells (RAMEC). Cell lysates (100 μg) were separated by SDS-PAGE, transferred to nitrocellulose, and probed with anti-VACM-1 antibody A (Ab A) specific against the amino terminus of VACM-1. *C*: proliferation of CHO and the clone A cell line expressing VACM-1 cDNA. Cells were seeded at equal density, and their proliferation was determined after 72 h ($n = 6$, $^*P < 0.05$). *D*: flow cytometry analysis of control and VACM-1-transfected CHO cells. Cells grown to semiconfluence were arrested with 1.25 μM aphidicolin. After 16 h, cells were released and harvested at 0, 4, 8, 12, and 24 h, their DNA was stained with propidium iodide, and their progression through the cell cycle was monitored by fluorescence-activated cell sorting (FACS) analysis.

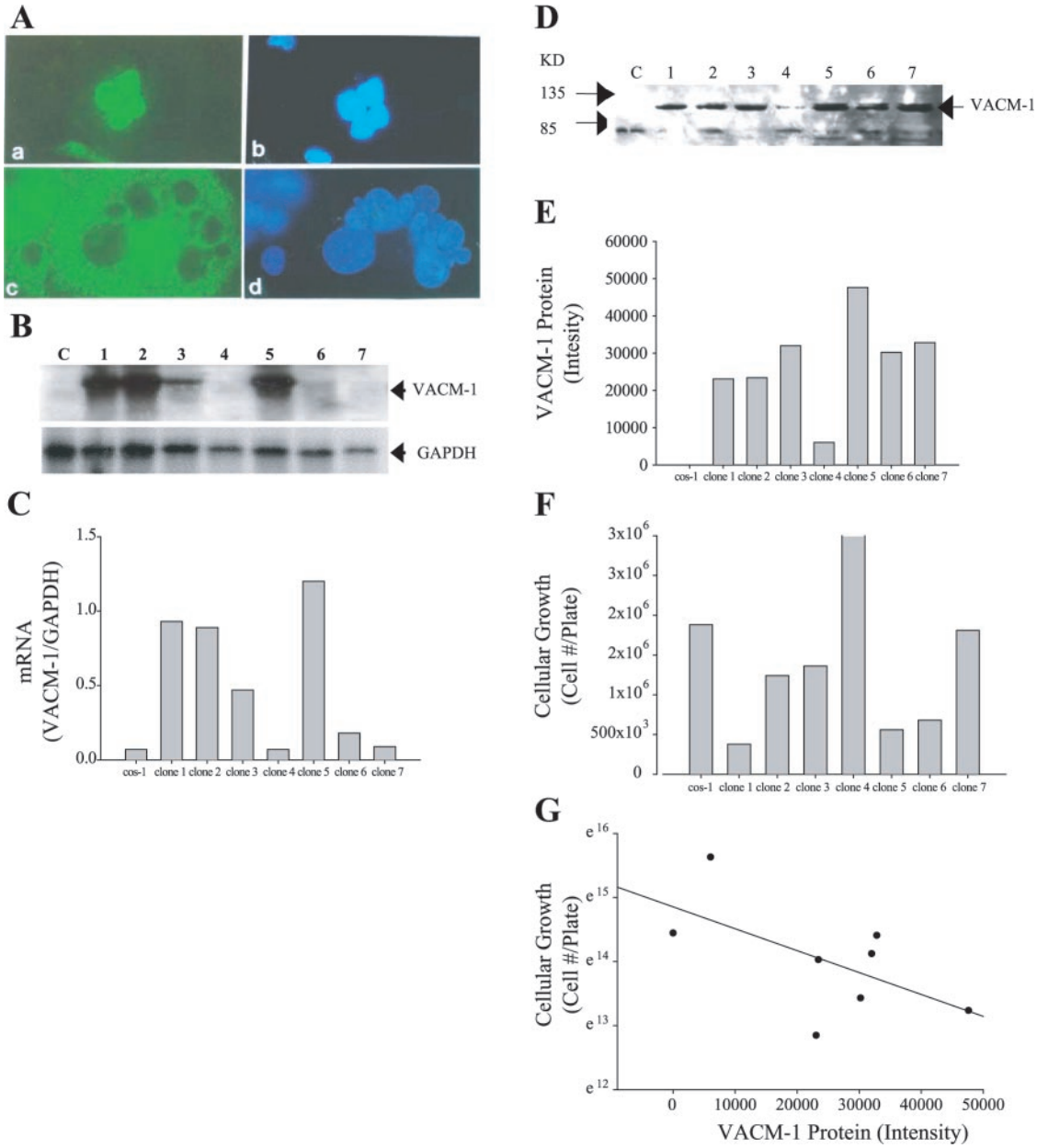


Fig. 2. Effects of VACM-1 cDNA expression in COS 1 cells. *A*: immunocytochemical staining of VACM-1 stably transfected COS-1 cells with anti-VACM-1-specific antibodies. *a* and *c*: immunostaining of cultures with an antibody generated against the carboxyl terminus of VACM-1 (Ab B). *b* and *d*: 4,6-diamidino-2-phenylindole (DAPI) nuclear staining of cells shown in *a* and *c*, respectively. No VACM-1 expression was observed in cells immunostained with the antibody preincubated with 10 μg of peptide (data not shown). Cells were grown on coverslips, fixed, permeabilized, and immunostained with anti-VACM-1 antibody. Magnification, ×40. *B* and *C*: poly(A^+) mRNA from control and 7 clones was isolated and separated for Northern blot analysis. Blots were hybridized with the ^{32}P-labeled *Eco*RI/*Bcl*I fragment from VACM-1 cDNA (*B*, *top*). The blot was reprobed with anti-GAPDH probe (*bottom*), and the intensity of the mRNA signal was quantified and corrected for uneven RNA loading (*C*). *D* and *E*: Western blot analysis of COS-1 stably derived cell lines expressing VACM-1 protein. Total cell lysate protein (100 μg) was run on SDS-PAGE and transferred to a nitrocellulose membrane. The blots were probed with antibodies against the amino terminus (Ab A) of VACM-1. After incubation with horseradish peroxidase-linked secondary antibody, blots were visualized by using a chemiluminescent reagent (*D*) and signal intensity was quantitated (*E*). *F*: growth rates of COS-1 VACM-1 stably transfected clonal lines. COS-1-derived clones were seeded at equal density (5×10^4 cells/plate), and their growth was monitored over time. *G*: correlation between cell growth and VACM-1 protein levels ($r = 0.68$, $P < 0.05$).

but failed to undergo complete cytokinesis (Fig. 2*A*, *c–d*). No VACM-1 staining was observed in CMV vector-transfected control cells (data not shown). Five additional clones, originally selected at random, were lost as they failed to progress beyond the stage shown in Fig. 2*A*. These observations were confirmed by subsequent Northern and Western blot analyses. Essentially, no VACM-1 expression could be detected in the

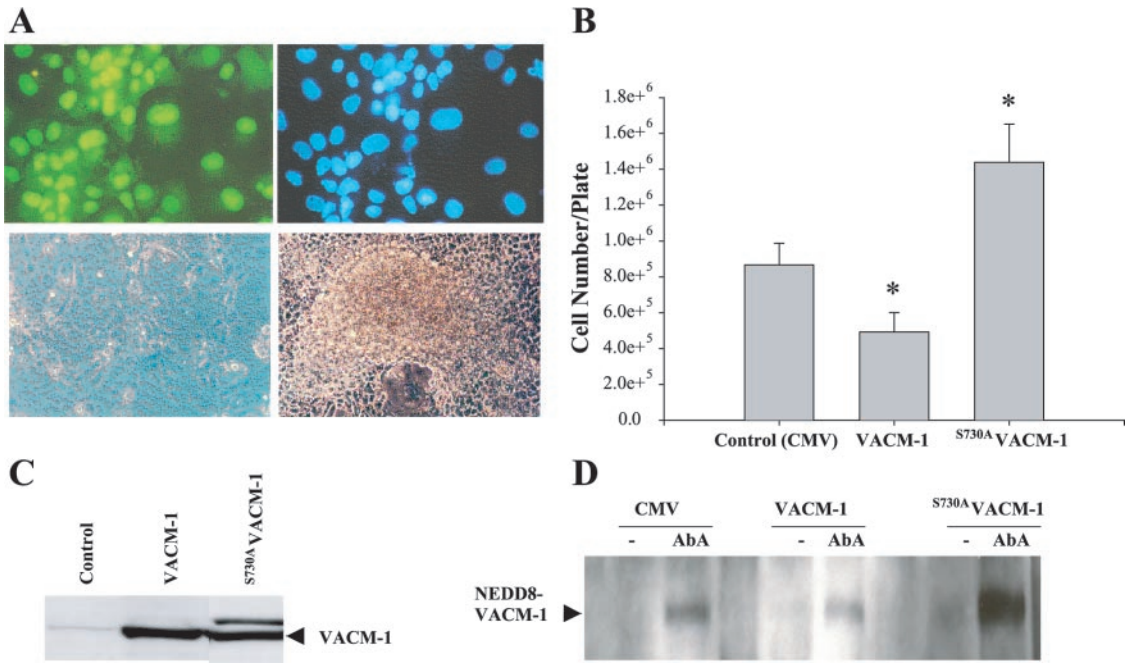


Fig. 3. Effects of ^{S730A}VACM-1 expression in COS-1 cells. *A*: immunocytochemical staining and light microscopy of COS-1 cells stably transfected with ^{S730A}VACM-1 cDNA mutant. COS-1 cells expressing ^{S730A}VACM-1 protein grown to different levels of confluency were immunostained with anti-VACM-1 Ab A (*a*) and counterstained with DAPI (*b*). *c* and *d*: representative phase-contrast microscopy of vector- and ^{S730A}VACM-1 cDNA-transfected cells, respectively. Essentially the same results were obtained in at least 5 independent clones examined. Cells were grown on coverslips, fixed, permeabilized, and immunostained. Magnification: *a* and *b*, ×40; *c* and *d*, ×10. *B*: CMV vector-, VACM-1-, and ^{S730A}VACM-1 cDNA-transfected cells were seeded at equal density (5×10^4 cells/plate), and their growth was monitored ($n = 4$, $^*P < 0.05$ compared with control). *C*: Western blot analysis of cell lysates from CMV vector-, VACM-1-, and ^{S730A}VACM-1-transfected cells with anti-VACM-1 Ab A was performed as described in Fig. 2*D*. *D*: cell lysates from CMV vector-, VACM-1-, and ^{S730A}VACM-1 cDNA-transfected cells were immunoprecipitated with anti-VACM-1 antibody (Ab A) or a nonspecific antibody (−), separated by SDS-PAGE, transferred to nitrocellulose, and probed with anti-NEDD8 antibody.

control cells, whereas varied concentrations of both VACM-1 mRNA (Fig. 2, *B–C*) and VACM-1 protein (Fig. 2, *D–E*) were detected in the selected cell lines. To examine the effect of VACM-1 expression on growth rates, COS-1-derived cell lines expressing VACM-1 were seeded at the same density, harvested at specific time points, and counted. Representative data, shown in Fig. 2*F*, indicate that all but *clone 4* cells, which had the lowest VACM-1 mRNA and protein levels (Fig. 2, *B–E*), grew at a much lower rate than the control COS-1 cells (CMV transfected). Furthermore, cellular growth rates were inversely and significantly correlated to VACM-1 protein concentrations (Fig. 2*G*, $r = 0.68$, $P < 0.05$).

Because we have shown previously that mutation of the PKA-dependent phosphorylation site in VACM-1 sequence (S730A) reversed the attenuating effect of VACM-1 expression on cAMP production (2), we asked whether expression of ^{S730A}VACM-1 mutant would affect cellular growth. Unlike the VACM-1-derived lines described above, all 12 lines expressing ^{S730A}VACM-1 protein grew rapidly compared with several CMV vector-transfected control lines (data not shown). Immunocytochemistry and light microscopy data indicate that these cells appeared to lose contact inhibition, and unlike control cells, which stopped growing as they reached confluency (Fig. 3*Ac*), ^{S730A}VACM-1 cDNA-transfected cells continued to grow and formed foci (Fig. 3*A*, *a*, *b*, and *d*). The growth rates for the representative lines from control, CMV, VACM-1, and ^{S730A}VACM-1 COS-1 cells were quantified and are shown in Fig. 3*B*. Clearly, VACM-1-transfected cells had significantly lower growth rates compared with the vector-transfected cells ($n = 4$, $P < 0.05$), whereas ^{S730A}VACM-1-expressing cells had significantly higher growth rates compared with either the vector- or VACM-1-transfected groups ($n = 4$, $P < 0.05$). Western blot analysis with antibodies directed against either the carboxyl terminus (Fig. 3*C*) or the amino terminus (see Fig. 5) of VACM-1 protein confirmed the presence of VACM-1 protein in cells transfected with ^{S730A}VACM-1 cDNA. Interestingly, in all ^{S730A}VACM-1-derived lines, an additional protein band was visible in blots probed with antibodies directed against either the amino or the carboxyl terminus of VACM-1 protein (Fig. 5*A* and Fig. 3*C*, respectively). To identify this modification, cell lysates from CMV-, VACM-1-, and ^{S730A}VACM-1 cDNA-transfected cells were immunoprecipitated with the antibody directed against the amino terminus of VACM-1 protein (Ab A) and separated by SDS-PAGE for Western blot analysis with an antibody directed against NEDD8 protein, previously

shown to modify cullins (14, 31, 33). Although preliminary, our results indicate that anti-NEDD8 antibody recognizes protein immunoprecipitated with Ab A from ^{S730A}VACM-1 cDNA-transfected COS-1 cells. A weak signal was also detected in the CMV- and VACM-1 cDNA-transfected cell lysates incubated with Ab A. No signal was detected in any of the samples immunoprecipitated with a nonspecific antibody (Fig. 3*D*).

To examine whether MAPK phosphorylation was compromised in control and in CMV-, VACM-1-, and ^{S730A}VACM-1-transfected cells, Western blot analyses of cell lysates from control and VACM-1-transfected cells were performed using anti-MAPK and anti-phospho-p44/p42 MAPK-specific antibodies. The results from the control and VACM-1-transfected CHO cells are shown in Fig. 4*A*. The signal intensity of phosphorylated (P)-MAPK and a 44-kDa MAPK (ERK2) was increased in CHO cells treated with 10% FBS (Fig. 4*A*, *top* and *bottom*, respectively). In clone A cells expressing VACM-1, a small increase in MAPK (Fig. 4*A*, *bottom*) but not in P-MAPK levels (*top*) could be detected in response to FBS. Furthermore, no P-MAPK signal was observed in unstimulated clone A cells (Fig. 4*A*, *top*). AVP (1 μM) had no effect on MAPK phosphorylation in either the control or VACM-1-transfected cells. Similar observations were made in the COS-1-derived cell line, where VACM-1 protein expression prevented MAPK phosphorylation compared with the control cells (Fig. 4*B*, $n = 3$, $P < 0.05$). The expression of ^{S730A}VACM no longer prevented MAPK phosphorylation. To confirm equal protein loading, blots were stripped and reprobed with anti-α-actin antibody. To examine whether there exists a correlation between the degree of MAPK phosphorylation and ^{S730A}VACM protein levels, cell lysates from clones expressing varied levels of ^{S730A}VACM-1 were first probed with the antibody directed against the amino terminus of VACM-1 protein, stripped, and reprobed with anti-P-MAPK antibody. To confirm equal protein loading, blots were reprobed with an anti-tubulin antibody. These data, summarized in Fig. 5*A*, indicate that ^{S730A}VACM-1 cDNA-transfected cells express VACM-1 protein and a larger molecular weight protein (*top*), identified in Fig. 3*D* as NEDD8-conjugated VACM-1. Whereas there was no detectable MAPK phosphorylation in VACM-1-transfected cells, phosphorylated p42 and p44 MAPK was detected in all ^{S730A}VACM-1 cDNA-transfected cell lines (Fig. 5*A*, *middle*). Interestingly, the degree of p42 and p44 MAPK phosphorylation was dependent on the levels of the modified VACM-1 protein (Fig. 5*B*, $r^2 = 0.668$).

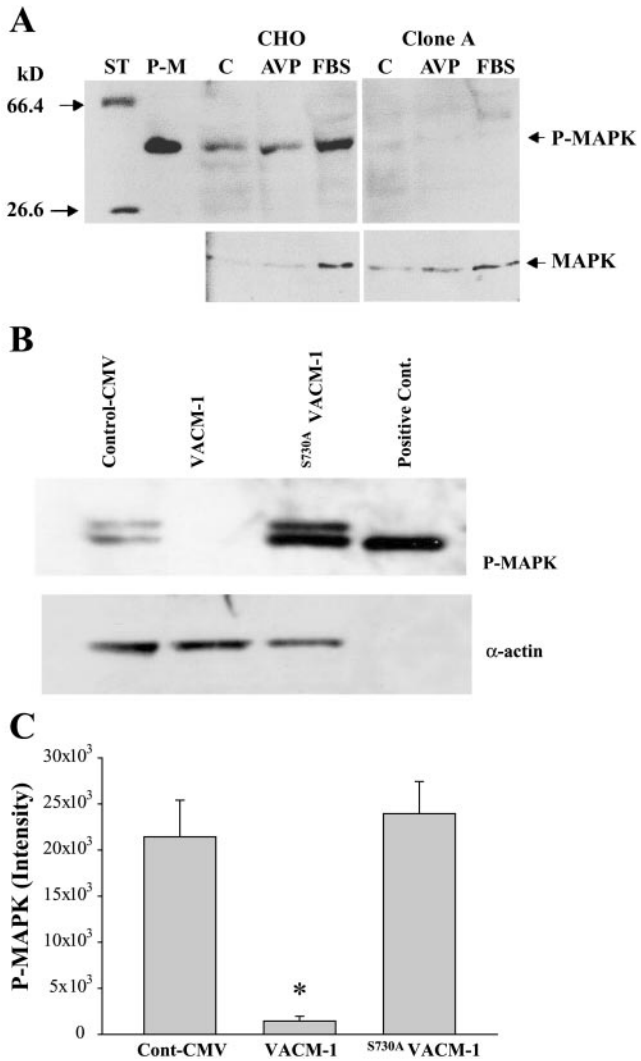


Fig. 4. Effects of VACM-1 and ^{S730A}VACM-1 mutant on MAPK phosphorylation in representative CHO and COS-1 clonal cell lines. *A*: MAPK and phosphorylated MAPK levels in CHO cells and CHO cells expressing VACM-1 cDNA. Cell lysates (25 μg) from control (C) and AVP (10^{-6} M)- and FBS (10%)-treated CHO and clone A cells were separated by SDS-PAGE and probed with MAPK antibody that recognizes only the phosphorylated MAPK (P-MAPK; *top*) or the total MAPK (*bottom*). P-M, phosphorylated MAPK control sample; ST, molecular weight markers. *B*: Western blot analysis of P-MAPK protein levels in control and VACM-1-, CMV vector-, and ^{S730A}VACM-1-transfected COS-1 cells. Total cell lysate proteins (50 μg) were run on SDS-PAGE gel, transferred to nitrocellulose membrane, and probed with anti-P-MAPK antibody (*top*). Blots were reprobed with anti-α-actin to correct for unequal protein loading (*bottom*). *C*: intensity of the signal was quantified using NIH Scion Imaging ($n = 3$, $^*P < 0.05$).

To identify steps subsequent to MAPK phosphorylation in the VACM-1-dependent cellular signaling system, we performed a screening analysis with a Human PathwayFinder-1 GEArray. Our data indicate that of the 24 genes present on the blot, 5 appeared to be affected by VACM-1 overexpression (Fig. 6*A*). Interestingly, the only gene induced by VACM-1 was p53, whereas creb-2, egr-1, hsf1, and hsp90 were decreased compared with the vector-transfected control cells. To confirm the GEArray analysis results at the protein level, we immunostained COS-1 control (CMV vector), VACM-1, and ^{S730A}VACM-1 stably transfected cells with anti-p53 antibody. As shown in a representative experiment in Fig. 6*B* ($n = 3$), the immunostaining with anti-p53-specific antibody demonstrated increased nuclear fluorescence intensity in VACM-1-transfected COS-1 cells compared with CMV control and ^{S730A}VACM-1-transfected cells. These observations were further confirmed by Western blot analyses of cell lysates from CMV control, VACM-1-transfected,

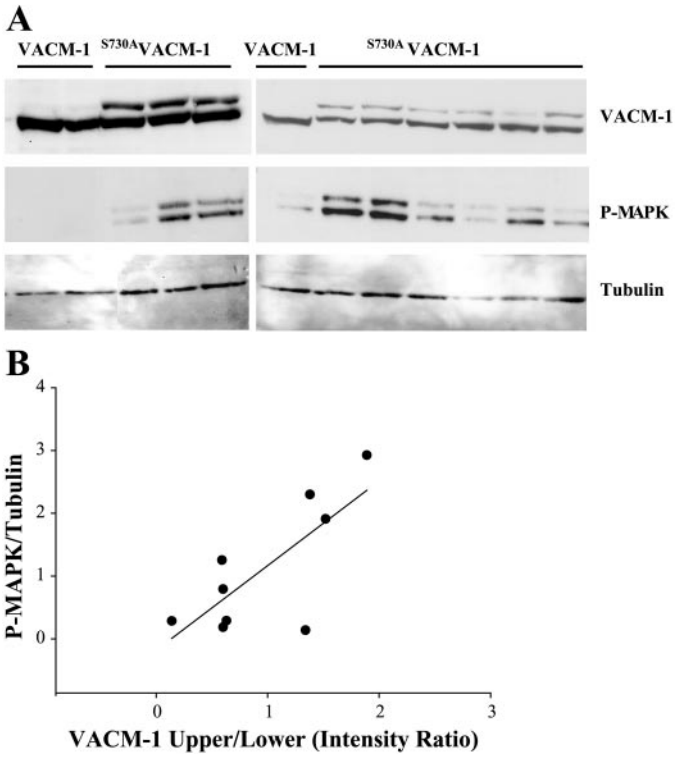


Fig. 5. Effects of ^{S730A}VACM-1 expression on MAPK phosphorylation in COS-1 cells. *A*: total cell lysate proteins (50 μg) from VACM-1- and ^{S730A}VACM-1-transfected COS-1 cells were run on SDS-PAGE gel and transferred to nitrocellulose membrane. Blots were probed with antibody generated against the amino terminus of VACM-1 (*top*), stripped, and reprobed with anti-P-MAPK antibody (*middle*). To correct for unequal protein loading, blots were reprobed with anti-tubulin antibody (*bottom*). *B*: intensity of the signal for each blot was quantified using NIH Scion Imaging, and P-MAPK/tubulin signal was plotted against VACM-1 protein intensity (*top* vs. *bottom bands*) ($r^2 = 0.668$).

and ^{S730A}VACM-1-transfected cells using anti-p53-specific antibody ($n = 3$) (Fig. 6, *C* and *D*). Interestingly, the significantly higher levels of p53 protein in VACM-1-transfected COS-1 cells compared with either the vector-transfected or ^{S730A}VACM-1-transfected cells were also associated with an increase in a higher molecular weight p53 species (Fig. 6, *C* and *D*).

DISCUSSION

VACM-1 protein shares sequence homology with cullins, suggesting a possible role as a cell cycle-regulating protein (6, 17, 21). When expressed in vitro, VACM-1 increases cytosolic free Ca^{2+} concentration and attenuates cAMP production (2, 4, 5). Because the cAMP pathway has been implicated in regulation of cellular proliferation in response to many growth factors (10, 18, 32), we extended our search for the function of VACM-1 protein in that direction. To investigate the effects of VACM-1 expression on cellular growth, we established several cell lines stably expressing VACM-1 cDNA. Both cell models, used extensively to characterize cellular and membrane proteins and signaling pathways, have been shown to express negligible levels of endogenous VACM-1 (2, 4). Our results indicate that VACM-1 attenuates cellular growth when expressed in both CHO and COS-1 cells (Fig. 1, *A* and *C*, and Fig. 2, *A*, *F*, and *G*, respectively). Furthermore, FACS and immunocytochemistry analyses of CHO cells expressing VACM-1 protein suggest that cells expressing VACM-1 progress through the cell cycle at a slower rate than the control CHO cells (Fig. 2). Importantly, our work demonstrates that expression of VACM-1 protein prevents phosphorylation of MAPK and leads to an increase in p53 mRNA and protein levels (Figs. 4–6), signaling molecules well recognized for their role in the regulation of cellular growth (1, 10, 18).

This mechanism for the VACM-1-dependent regulation of cellular growth is supported by recent reports implicating cullins in the regulation of both MAPK activity and p53 levels (23, 28). For example, in *Dictyostelium,* the PKA/cAMP-dependent signaling important in the regulation of development is regulated by cullins (23). In this system, the ERK2-dependent phosphorylation of cAMP-specific phosphodiesterase, RegA, is required for the phosphodiesterase to be recognized by ubiquitin-proteosome complex containing a cul-1 homolog, CulA (23). CulA-null cells are defective in inducing cell type-specific gene expression and exhibit defects during aggregation (23). Similarly, Querido et al. (28) have reported that to permit efficient viral replication, adenovirus E1B55K and E4orf6 proteins complex with cul-5 containing ubiquitin ligase and promote degradation of p53 in vitro (28). The observation that VACM-1 expression increased levels of modified p53 (Fig. 6*C*, *top band*) also suggests that VACM-1 may regulate p53 levels at the posttranslational level.

The human VACM-1 gene has been localized on chromosome 11q22–23 to a region close to the gene for ataxia telangiectasia (ATM) and associated with a loss of heterozygosity in breast cancer tumor samples (6, 16). Because loss of ATM gene product slows the induction of p53 in response to DNA breaks, VACM-1 has been suggested as a possible tumor suppressor gene (6). We have reasoned, therefore, that if VACM-1 expression is critical to the regulation of cellular growth (see above), creating a dominant negative phenotype of VACM-1 would reverse this effect. We first chose to study the ^{S730A}VACM-1 mutant, which, when expressed in COS-1 cells, no longer inhibits cAMP production (2). Our data indicate that overexpression of ^{S730A}VACM-1 mutant leads to a significant increase in cellular proliferation compared with the CMV vector-transfected control lines. Importantly, the expression of ^{S730A}VACM-1 mutant no longer inhibited the phosphorylation of MAPK observed in cells overexpressing VACM-1 protein (Fig. 4). Furthermore, Western blot analysis data indicate that phosphorylation of MAPK in ^{S730A}VACM-1 mutant lines was dependent on the levels of NEDD8-modified VACM-1 protein (Fig. 5*A*, *top band*).

It is now apparent that all cullins may be modified by NEDD8 (20, 30–32), a novel regulator of proteolytic targeting by ubiquitination (14, 20). In *Schizosaccharomyces pombe*, increased neddylation of cul-1 homo-

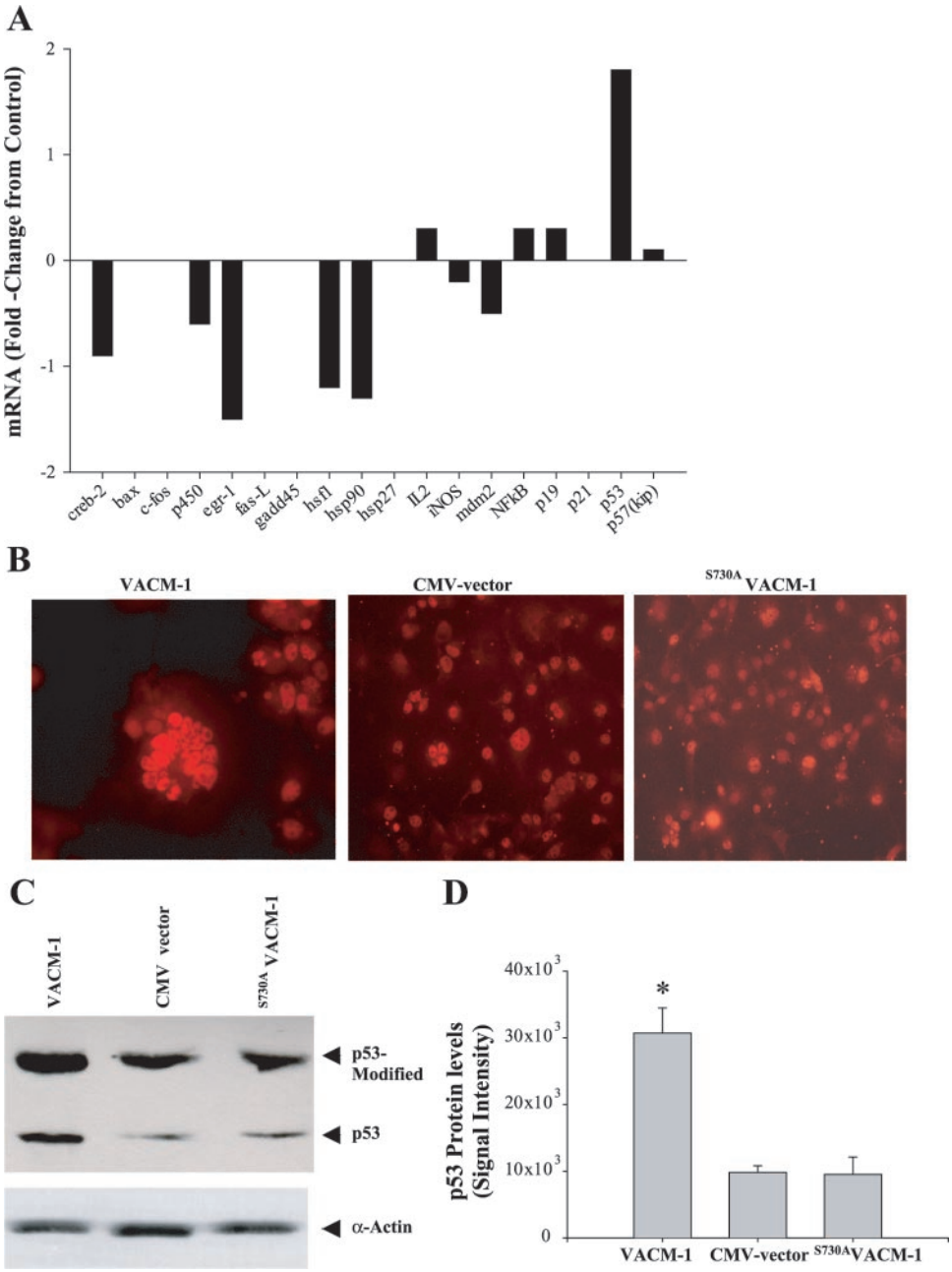


Fig. 6. Effects of VACM-1 expression on gene RNA and protein induction in COS-1 cells. *A*: Human PathwayFinder GEArray was probed with cRNA derived from vector-transfected control COS-1 cells and from VACM-1 cDNA-transfected cell line 1. Data were corrected for GAPDH mRNA and are expressed as a ratio of *clone 1* to control cells. *B*: immunocytochemical staining of VACM-1-transfected (*a*), control (CMV vector-transfected only; *b*), and ^{S730A}VACM-1 mutant-transfected COS-1 cells (*c*) with an anti-p53 antibody. *C*: representative Western blot analysis of p53 protein in VACM-1-, CMV vector-, and ^{S730A}VACM-1-transfected COS-1 cells. Total cell lysate proteins (50 μg) were run on SDS-PAGE gel, transferred to nitrocellulose membrane, and probed with anti-p53 antibody (*top*). Equal protein loading was confirmed by reprobing blots with an anti-α-actin antibody (*bottom*). *D*: intensity of the signal shown in *C* was quantified using NIH Scion Imaging ($n = 3$, $^*P < 0.05$).

logue in the SCF ubiquitin ligase complex led to increased ubiquitynylase activity. In cells deficient in the neddylation machinery, the half-life of the SCF substrate was not affected, however, indicating that unlike ubiquitinylation, NEDD8 conjugation does not target proteins for degradation (20). Furthermore, mutation in the NEDD8-activating enzyme caused yeast cells to undergo multiple S phases without intervening mitosis (14), and in U2OS and HEK-293 cells, this mutation compromised cell cycle transitions and inhibited cell growth (30). Interestingly, the ts41 mutation in CHO cells, which leads to successive S phases in the absence of the intervening mitosis (12), is apparently a result of inactivation of the *SMC1* gene encoding for a subunit of the NEDD8-activating enzyme (12, 14, 30). Whether the apparent phenotype similarity of clone A overexpressing VACM-1 (cul-5) protein, which appears to undergo successive S phases in the absence of the mitosis (Fig. 2*A*), to the ts41 mutant results from the inability of NEDD8 to modify VACM-1 remains to be established.

The NEDD8 conjugation region has been localized to Lys^{689} in cul-2 (Lys^{724} in VACM-1) and is highly conserved in all cullins (31). Interestingly, VACM-1 protein sequence analysis (**AI**IQ**IMKMRK**KL**S**) revealed that the NEDD8 conjugation region (bold) overlaps the PKA-dependent phosphorylation site (underlined), ^{727}KKL**S**^{730} (4), which is not conserved in other cullins (31). This difference may explain poor neddylation of cul-5 (31). When Ser^{730} in the VACM-1 protein se-

quence was mutated to Ala, it conferred upon VACM-1 the ability to induce phenotype reversal (Fig. 3B) and to modify its structure (Figs. 3*C* and 5). Furthermore, the immunoprecipitation results suggest that both CMV- and VACM-1-transfected cells may express low levels of neddylated VACM-1 protein (Fig. 3*D*) not detected by a Western blot analysis (Fig. 3*C*). Lyapina et al. (20) have proposed that NEDD8 may need to be cyclically attached to and cleaved from cul-1 for the optimal function of SCF complex. Whether a similar mechanism may take place in the VACM-1-dependent regulation of cellular function remains to be established. The observation that the level of MAPK-1 phosphorylation is dependent on the ratio of modified to unmodified VACM-1 supports this hypothesis.

Finally, the Pathfinder analysis suggests that egr-1 and heat shock genes hsf1 and hsp90, but not hsp70 or hsp27, were also affected in cells overexpressing VACM-1 protein. Because mitogens, growth factors, and tumor promoters that induce cellular proliferation by transcriptional activation of the egr-1 gene involve the PKA-dependent phosphorylation of cytosolic ERK and nuclear CREB (cAMP response element binding) proteins (18), it is possible that VACM-1-dependent attenuation of cAMP concentration (5) and the subsequent inhibition of MAPK phosphorylation (Fig. 4) may be responsible for the decrease in egr-1 mRNA expression. Heat shock protein genes can be induced by diverse conditions and act as a safeguard mechanism to ensure survival of the stressed cells (7). Hsp90, for example, plays an essential role in stress tolerance, protein folding, and posttranslational stability and function of many proteins involved in the regulation of cell growth and differentiation (24). It is thus possible that VACM-1-dependent inhibition of their expression may also contribute to the observed attenuation of cellular growth.

In summary, cell cycle-specific expression of VACM-1 protein and its regulation of cAMP and Ca^{2+} signaling pathways, MAPK phosphorylation and regulation of p53 gene expression, and, ultimately, cellular growth raise interesting possibilities. When localized to the nucleus, VACM-1 may regulate the abundance/activity of cell cycle regulatory molecules and cytokinesis. When localized to the cell membrane, it may regulate cAMP-dependent signaling pathways that will affect growth. Although the VACM-1 nuclear localization signal sequence has been identified (6), it lacks a clear membrane signal peptide sequence (4). Consequently, the mechanism of its translocation to the cell membrane is not known. It is possible that, like other cullin gene products (27), VACM-1 forms complexes with some regulatory proteins, which may help its translocation to the cell membrane. Consequently, VACM-1 may be the link between the cytosolic/nuclear signaling pathways and the extracellular events, which may result in diminished cellular growth and/or increased cellular death. Further studies are required to delineate the mechanism and the significance of the cell cycle-specific translocation of VACM-1 to the cell membrane and/or nucleus and its role in suppression of cellular growth.

We acknowledge Dr. C. Barney (Hope College) for helpful suggestions in preparing this manuscript.

DISCLOSURES

This work was supported by National Institute of Diabetes and Digestive and Kidney Diseases Grant R01-DK-47199, National Science Foundation-Research Experiences for Undergraduate Grants DBI-982057 and CHE-9619667, The Camille and Henry Dreyfus Foundation Award (to M. Burnatowska-Hledin), and a Pfizer Co. grant (to J. Kossoris).

REFERENCES

1. **Agarwal M, Taylor W, Chernov M, Chernova O, and Stark G.** The p53 network. *J Biol Chem* 273: 104–108, 1998.
2. **Burnatowska-Hledin M, Capps B, Folta V, Zhao P, Mungall C, Sharangpani AM, and Listenberger L.** VACM-1, a cullin gene family member, regulates cellular signaling. *Am J Physiol Cell Physiol* 279: C266–C273, 2000.
3. **Burnatowska-Hledin M, Lazdins IB, Listenberger L, Zhao P, Sharangpani A, Folta V, and Card B.** VACM-1 receptor is specifically expressed in rabbit vascular endothelium and renal collecting tubule. *Am J Physiol Renal Physiol* 276: F199–F209, 1999.
4. **Burnatowska-Hledin M, Spielman WS, Smith WL, Shi P, Meyer JM, and Dewitt DL.** Expression cloning of an AVP-activated calcium-mobilizing receptor from rabbit kidney medulla. *Am J Physiol Renal Fluid Electrolyte Physiol* 268: F1198–F1210, 1995.
5. **Burnatowska-Hledin M, Zeneberg A, Roulo A, Grobe J, Zhao P, Lelkes PL, Clare P, and Barney C.** Expression of VACM-1 protein in cultured rat adrenal endothelial cells is linked to the cell cycle. *Endothelium* 8: 49–63, 2001.
6. **Byrd PJ, Stankovic T, McConville CM, Smith AD, Cooper PR, and Taylor AMR.** Identification and analysis of expression of human VACM-1, a cullin gene family member located on chromosome 11q22–23. *Genome Res* 7: 2–6, 1997.
7. **Caruccio L, Bae S, Liu AY, and Chen, KY.** The heat-shock transcription factor HSF-1 is rapidly activated by either hyper- or hypo-osmotic stress in mammalian cells. *Biochem J* 327: 341–347, 1997.
8. **Chen L, Manjeshwar S, Lu Y, Moore D, Ljung BM, Kuo WL, Dairkee SH, Wernick M, Collins C, and Smith HS.** The human homologue for the *Caenorhabditis elegans* cul-4 gene is amplified and overexpressed in primary breast cancers. *Cancer Res* 58: 3677–3683, 1998.
9. **Du M, Sansores-Garcia L, Zu Z, and Wu KK.** Cloning and expression analysis of a novel salicylate suppressible gene, HsCUL3, a member of cullin/Cdc53 family. *J Biol Chem* 273: 24289–24292, 1998.
10. **Dumont JE, Jauniaux JC, and Roger PP.** The cyclic AMP-mediated stimulation of cell proliferation. *Trends Biochem Sci* 14: 67–71, 1989.
11. **Grossberger R, Gieffers C, Zachariae W, Podtelejnikov AV, Schleiffer A, Nasmyth K, Mann M, and Peters JM.** Characterization of the DOC1/APC10 subunit of the yeast and the human anaphase-promoting complex. *J Biol Chem* 274: 14500–14507, 1999.
12. **Handeli S and Weintraub H.** The ts41 mutation in Chinese hamster cells leads to successive S phases in the absence of intervening G_2, M, and G_1. *Cell* 71: 599–611, 1992.
13. **Handler JS and Orloff J.** Antidiuretic hormone. *Annu Rev Physiol* 43: 611–624, 1981.
14. **Hori T, Osaka F, Chiba T, Miyamoto C, Okabayashi K, Shimbara N, Kato S, and Tanaka K.** Covalent modification of all members of human cullin family proteins by NEDD8. *Oncogene* 18: 6829–6834, 1999.
15. **Kamura T, Koepp DM, Conrad MN, Skowyra D, Moreland RJ, Iliopoulos O, Lane WS, Kaelin WG Jr, Elledge SJ, Conaway RC, Harper JW, and Conaway JW.** Rbx1, a com-

ponent of the VHL tumor suppressor complex and SCF ubiquitin ligase. *Science* 284: 657–661, 1999.
16. **Kastan MB, Qimin-Zhan WS, El-Deiry FC, Jacks T, Walsh WV, Plunkett BS, Vogelstein B, and Fornace A Jr.** A mammalian cell cycle checkpoint pathway utilizing p53 and GADD45 is defective in *Ataxia-talamgiectasia*. *Cell* 71: 587–597, 1992.
17. **Kipreos ET, Lander LE, Wing JP, He WW, and Hedgecock EM.** cul-1 is required for cell cycle exit in *C. elegans* and identifies a novel gene family. *Cell* 85: 829–839, 1996.
18. **Lalli E and Sassone-Corsi P.** Signal transduction and gene regulation: the nuclear response to cAMP. *J Biol Chem* 269: 17359–17362, 1994.
19. **Longeran KM, Iliopoulos O, Ohh M, Kamura T, Conaway RC, Conaway JW, and Kaelin WG Jr.** Regulation of hypoxia-inducible mRNAs by the von Hippel-Lindau tumor suppressor protein requires binding to complexes containing elongins B/C and Cul2. *Mol Cell Biol* 18: 732–741, 1998.
20. **Lyapina S, Cope G, Shevchenko A, Serino G, Tsuge T, Zhou C, Wolf DA, Wei N, Shevchenko A, and Deshaies RJ.** Promotion of NEDD8-CUL1 conjugate cleavage by COP9 signalosome. *Science* 292: 1382–1385, 2001.
21. **Mathias N, Johnson SL, Winey M, Adams AEM, Goetsch L, Pringle Byers B, and Goebl MG.** Cdc53p acts in concert with Cdc4p and Cdc34p to control the G_1-to-S-phase transition and identifies a conserved family of proteins. *Mol Cell Biol* 16: 6634–6643, 1996.
22. **Michel JJ and Xiong Y.** Human CUL-1, but not other cullin family members, selectively interacts with SKP1 to form a complex with SKP2 and cyclin A. *Cell Growth Differ* 9: 435–449, 1998.
23. **Mohanty S, Lee S, Yadava N, Dealy MJ, Johnson RS, and Fritel RA.** Regulated protein degradation controls PKA function and cell-type differentiation in Dictyostelium. *Genes Dev* 15: 1435–1488, 2001.
24. **Morano DA and Thiele D.** Heat shock factor function and regulation in response to cellular stress, growth, and differentiation signals. *Gene Expr* 7: 271–282, 1999.
25. **Mukhopadhyay D, Knebelmann B, Cohen HT, Ananth S, and Sukhatme VP.** The von Hippel-Lindau tumor suppressor gene product interacts with Sp1 to suppress vascular endothelial growth factor promoter activity. *Mol Cell Biol* 17: 5629–5639, 1997.
26. **Papadimitriou E, Unsworth BR, Maragoudakis ME, and Lelkes PI.** Time-course and quantification of extracellular matrix maturation in the chick chorioallantoic membrane and in cultured endothelial cells. *Endothelium* 1: 207–219, 1993.
27. **Pause A, Lee S, Worrell RA, Chen DYT, Burgess WH, Linehan WM, and Klausner RD.** The von Hippel-Lindau tumor-suppressor gene product forms a stable complex with human CUL-2, a member of the Cdc53 family of proteins. *Proc Natl Acad Sci USA* 94: 2156–2161, 1997.
28. **Querido E, Blanchette P, Yan Q, Kamura T, Morrison M, Boivin D, Kaelin WG, Conaway RC, Conaway JW, and Branton PE.** Degradation of p53 by adenovirus E4orf6 and E1B55K proteins occurs via a novel mechanism involving a Cullin-containing complex. *Genes Dev* 15: 3104–3117, 2001.
29. **Stein GS, Stein JL, Lian JB, Last TJ, Owen T, and McCabe L.** *Synchronization of Normal Diploid and Transformed Mammalian Cells in Cell Biology: A Laboratory Handbook*, edited by Celis JE. New York: Academic, 1994, vol. 1.
30. **Wada H, Yeh ETH, and Kamitani T.** A dominant-negative UBC12 mutant sequesters NEDD8 and inhibits NEDD8 conjugation in vivo. *J Biol Chem* 275: 17008–17015, 2000.
31. **Wada H, Yeh ETH, and Kamitani T.** identification of NEDD8-conjugation site in human cullin-2. *Biochem Biophys Res Commun* 257: 100–1005, 1999.
32. **Walsh DA and Van Patten SM.** Multiple pathway signal transduction by the cAMP-dependent protein kinase. *FASEB J* 8: 1227–1236, 1997.
33. **Wu K, Chen A, and Pan ZQ.** Conjugation of Nedd8 to CUL1 enhances the ability of the ROC1-CUL1 complex to promote ubiquitin polymerization. *J Biol Chem* 275: 32317–32324, 2000.
34. **Yu H, Peters JM, King RW, Page AM, Hieter P, and Kirschner MW.** Identification of a cullin homology region in a subunit of the anaphase-promoting complex. *Science* 279: 1219–1222, 1998.
35. **Zachariae W, Shevchenko A, Andrews PD, Ciosk R, Galova M, Stark MJ, Mann M, and Nasmyth K.** Mass spectrometric analysis of the anaphase-promoting complex from yeast: identification of a subunit related to cullins. *Science* 279: 1216–1219, 1998.